Bioorganic & Medicinal Chemistry 27 (2019) 240–246

Contents lists available at ScienceDirect

Bioorganic & Medicinal Chemistry

journal homepage: www.elsevier.com/locate/bmc

The effect of replacing the ester bond with an amide bond and of overall stereochemistry on the activity of daptomycin

Ryan Moreira, Ghufran Barnawi, David Beriashvili, Michael Palmer, Scott D. Taylor*

Department of Chemistry, University of Waterloo, 200 University Avenue West, Waterloo, Ontario N2L 3G1, Canada

ABSTRACT

Daptomycin, a cyclic lipodepsipeptide antibiotic, has been used clinically since 2003 to treat serious infections caused by Gram-positive bacteria. Although 37 years have passed since daptomycin's discovery, its mechanism of action is still debated. In this report, the effect of replacing the ester bond with an amide bond, and overall stereochemistry, on daptomycin's biological activity was examined. Two peptides were prepared in which the threonine4 residue in the active daptomycin analog, Dap-K6-E12-W13, was replaced with (2*S*,3*R*)-diaminobutyric acid ((2*S*,3*R*)-DABA) or its epimer (2*S*,3*S*-DABA) converting the ring-closing ester bond to an amide bond. Both of these peptides were found to be considerably less active than Dap-K6-E12-W13. These results, along with our previous studies on other daptomycin analogs, enabled us to conclude that the ester bond is crucial to daptomycin's activity. *ent*-Dap-K6-E12-W13 was found to be at least 133-fold less active than Dap-K6-E12-W13, indicating that a chiral interaction with a chiral target is essential to daptomycin's activity. Studies examining the binding of Dap-K6-E12-W13 and *ent*-Dap-K6-E12-W13 to model liposomes consisting of phosphatidylglycerol (PG) and phosphatidylcholine suggest that the stereochemistry of PG plays a crucial role in daptomycin-membrane interactions.

1. Introduction

Daptomycin (Fig. 1) is a cyclic lipodepsipeptide antibiotic used clinically for treating infections caused by Gram-positive organisms.[1] Daptomycin-resistant bacteria have been slow to appear since it became broadly available in 2003, which has made daptomycin especially valuable for treating infections caused by multi-drug resistant Gram-positive bacteria. This particular characteristic of daptomycin has prompted the World Health Organization (WHO) to classify daptomycin as a last resort antibiotic, meaning that it should only be used for treating extreme cases such as life-threatening infections caused by multi-drug resistant bacteria.[2] Although resistance to daptomycin was slow to materialize initially, clinical isolates of daptomycin-resistant bacteria are now appearing with increasing frequency.[3] This is a cause for some concern: if widespread resistance to this last-resort antibiotic becomes prevalent then few, if any, alternatives are available.

It is known that daptomycin inserts into the bacterial membrane and the presence of phosphatidylglycerol (PG) in the bacterial membrane is required for activity.[4] It does not distribute within the cytoplasm.[5] How it exerts its antibacterial effect once it is bound to the membrane has been the subject of some debate. Some studies suggest that, upon inserting into the membrane, daptomycin oligomerizes and forms pores allowing small cations to enter or escape which results in the depolarization of the cell membrane and, consequently, cell death.[6–14] More recent studies suggest that daptomycin exerts its effect by aggregating in fluid membrane microdomains, which causes the dissociation of lipid II synthase (MurG) and phospholipid synthase (PlsX), two enzymes involved in bacterial cell wall synthesis and phospholipid synthesis, from the cytoplasmic side of the cell membrane, which causes cell envelope stress.[15] It is possible that daptomycin has a dual mechanism of action (MoA) in that it operates by both of these processes or even has another yet undiscovered action mechanism.[16]

One potentially powerful approach for uncovering daptomycin's MoA, and for producing novel antibiotics with improved properties, is by performing structure activity relationship (SAR) studies. However, daptomycin is a complex molecule, which has made the development of an efficient method for preparing daptomycin analogs a challenge.[17–19] Daptomycin consists of 13 amino acids, six of which are non-proteinogenic: D-Asn2, D-Ala8, D-Ser11, Orn6, (2*S*,3*R*)-methylglutamate (3MeGlu12), and kynurenine (Kyn13). Ten of these amino acids create the macrocyclic core, which is closed with a depsi-bond (ester bond) between the side chain of the threonine (Thr) residue at position 4 and the C-terminus of the kynurenine (Kyn) residue at position 13. The remaining three amino acids are part of a tripeptide attached to Thr4 and attached to the *N*-terminus of the Trp1 residue is a decanoic acid tail.

We recently developed a solid phase synthesis of daptomycin and have used this approach to prepare a variety of daptomycin analogs.[20–23] Among the analogs that we prepared was Dap-E12-W13, in which Kyn13 and the synthetically challenging MeGlu12 were

* Corresponding author.
E-mail address: s5taylor@uwaterloo.ca (S.D. Taylor).

https://doi.org/10.1016/j.bmc.2018.12.004
Received 4 October 2018; Received in revised form 27 November 2018; Accepted 4 December 2018
Available online 05 December 2018
0968-0896/

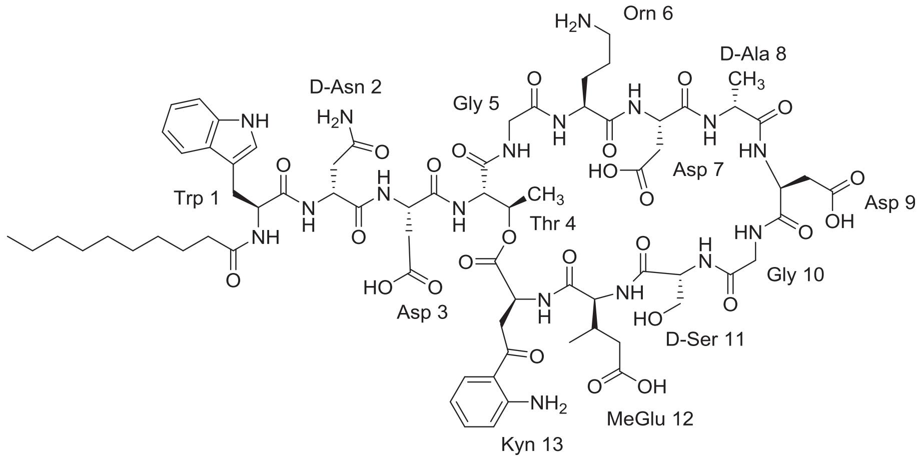

Fig. 1. Structure of daptomycin.

simultaneously replaced with Trp13 and Glu12, respectively.[20] This analog (MIC = 3.5 μg/mL) is only 4.6 fold less active against *B. subtilis* 1046 than daptomycin (MIC = 0.75 μg/mL) at physiological Ca^{+2} concentrations.[20,22] We have used this analog as a scaffold for performing SAR studies.[21,23] Very recently we have shown that Dap-K6-E12-W13, an analog in which all of the uncommon L-amino acids in daptomycin (Orn6, 3MeGlu12 and Kyn13) are replaced with their common counterparts (Lys6, Glu12 and Trp13), is only 2-fold less active than daptomycin with *B. subtilis* 1046 at physiological Ca^{+2} concentrations and over 2-fold more active that Dap-E12-W13.[23]

Among the questions for which we wished to answer with our SAR studies were: (1) can the ester bond in daptomycin be replaced with an amide bond without significant loss of activity? and, (2) what is the effect of overall stereochemistry on daptomycin's activity?

The answers to the above questions are of some interest. A study by D'Costa et al has shown that laboratory isolates of actinomycetes frequently attain resistance to daptomycin by enzymatic hydrolysis of the ester bond.[24] It is possible that this mechanism of resistance could be circumvented by replacing the ester bond with an amide bond. Moreover, it would be expected that the synthesis of such an analog would be less challenging since the formation of the ester bond is often the most difficult step in the chemical synthesis of daptomycin.[19,20]

Comparing both enantiomeric forms of biologically active peptides is a common tactic for determining whether or not the peptide is involved in a chiral interaction with a chiral target.[25a,b] Studying both enantiomeric forms of daptomycin or a reasonably active daptomycin analog, could determine whether or not a chiral interaction with a chiral target is essential to daptomycin's MoA.

Martin and coworkers attempted to answer the first question posed above by replacing Thr4 in Dap-E12-W13 with L-diaminopropionic acid (DAPA), thus replacing the ester bond with an amide bond (Dap-DAPA4-E12-W13).[26] As expected, this analog was much more resistant to degradation than daptomycin in human plasma serum; however, it was 82-fold less active (MIC = 160 μg/mL) against *S. aureus* than daptomycin (MIC = 1.9 μg/mL). It was suggested that the poor activity of Dap-DAPA4-E12-W13 was due to conformational changes/restrictions in the macrocycle that resulted from incorporation of the amide linkage.[26] However, we have found that Dap-S4-E12-W13, in which Thr 4 is replaced with Ser, was at least 29-fold less active (inactive up to 100 μg/mL) than Dap-E12-W13 against *B. subtilis*, indicating that the methyl group on the Thr4 side chain was very important for activity.[21] Therefore, the poor activity of Dap-DAPA4-E12-W13 may be due, in whole or in part, to the lack of a methyl group on the side chain of the DAPA residue rather than to the introduction of the new amide bond.

The Martin group also attempted to answer the second question by making the enantiomer of Dap-DAPA4-E12-W13 (*ent*-Dap-DAPA4-E12-W13).[26] They reported that *ent*-Dap-DAPA4-E12-W13 was inactive up to 1280 μM. On the basis of these results they suggested that a specific chiral interaction(s) may be required for daptomycin activity; however, due to the poor activity of Dap-DAPA4-E12-W13, it is not possible to draw a definitive conclusion concerning the effect of overall stereochemistry on the activity of daptomycin. What their results do reveal is that *ent*-Dap-DAPA4-E12-W13 is at least 8-fold less active than Dap-DAPA4-E12-W13. Indeed, since Dap-DAPA4-E12-W13 had such low activity and is probably structurally very different from daptomycin, it is even possible that this analog may not exert its antibacterial action by the same mechanism as daptomycin.

In this report, we provide more definitive answers to the above questions. This was achieved by preparing peptides **1** and **2** (Fig. 2), which are analogs of Dap-K6-E12-W13 in which Thr4 is replaced with (2*S*,3*R*)-diaminobutyric acid ((2*S*,3*R*)-DABA in peptide **1**) or its epimer (2*S*,3*S*-DABA in peptide **2**), as well as *ent*-Dap-K6-E12-W13. The biological activity of these peptides was determined and their interaction with model liposomes in the presence of Ca^{2+} studied.

2. Results and discussion

2.1. Syntheses

We elected to use Fmoc-protected (2*S*,3*R*)- or (2*S*,3*S*)-2-amino-3-

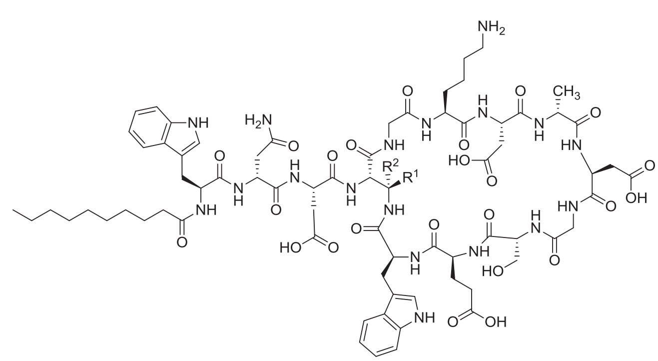

1, $R^1 = CH_3$, $R^2 = H$
2, $R^1 = H$, $R^2 = CH_3$

Fig. 2. Structures of peptides **1** and **2**.

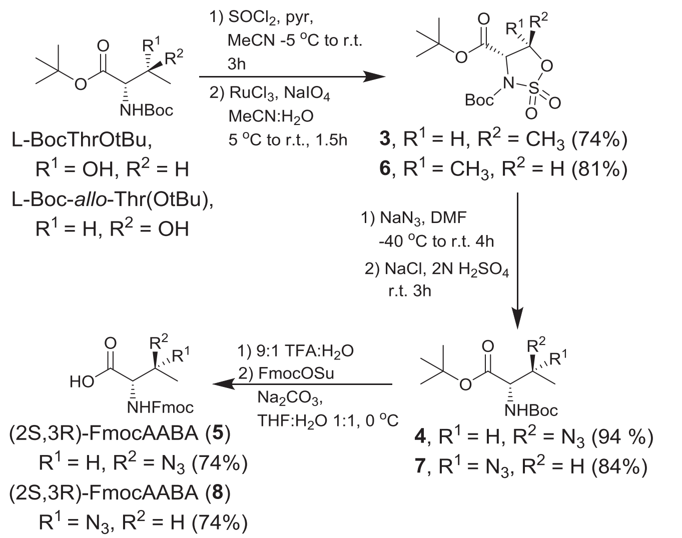

Scheme 1. Synthesis of (2*S*,3*R*)-FmocAABA (**5**) and (2*S*,3*S*)-FmocAABA (**8**).

azidobutanoic acid (FmocAABA) as building blocks for incorporating the DABA residues during Fmoc SPPS of peptides **1** and **2**. This strategy of using the azido group for protection of the β-amino group in DABA during Fmoc SPPS has recently been employed by Dianati et al. during the SPPS of a peptide-based protease inhibitor.[27] They prepared (2*S*,3*R*)- and (2*S*,3*S*)-FmocAABA via a 6-step synthesis starting from L-BocThr or L-Boc-*allo*-Thr.[27] Although this procedure was appealing, as it required only three chromatographic purifications, the overall yields were somewhat low (22–23%). Therefore, we decided to prepare these two isomers using a route similar to one that was described in a Pfizer patent for the synthesis of Boc-protected (2*S*,3*R*)-AABA benzyl ester.[28] As outlined in Scheme 1, BocThrOtBu[29] was converted to cyclic sulfamidate **3** through reaction with $SOCl_2$, followed by oxidation of the resulting sulfamidite with $NaIO_4$ catalyzed by $RuCl_3$. Compound **3** was opened by reaction with NaN_3 and the resulting sulfamic acid was hydrolyzed in a mildly acidic solution of aqueous sodium chloride to give compound **4**. The amino and COOH groups in **4** were deprotected using TFA:H_2O (9:1) and the α-amino group subsequently re-protected with FmocOSu, yielding (2*S*,3*R*)-FmocAABA (**5**). The same route was used to synthesize (2*S*,3*S*)-FmocAABA (**8**) starting from L-Boc-*allo*-ThrOtBu. The overall yields of this 6-step process, which required only one chromatographic purification (at the end of each synthesis), were 50% (for **5**) and 51% (for **8**).

With (2*S*,3*R*)-FmocAABA (**5**) and (2*S*,3*S*)-FmocAABA (**8**) in hand, we then prepared peptides **1** and **2** using the route outlined in Scheme 2 (synthesis of peptide **1** shown). Peptide **9**[23] was elongated by Fmoc-SPPS using HCTU/NMM to give peptide **10**. The azido moiety in peptide **10** was reduced using DTT/DIPEA in anhydrous DMF to give peptide **11**. Reducing the secondary azide using PMe_3 in 2:1 dioxane:H_2O produced the corresponding secondary alcohol, likely through phosphine-mediated diazonium formation.[30] The final three residues – Trp13, Glu12 and D-Ser11 – were coupled on to peptide **11** using DIC/HOBt to give peptide **12**. The alloc group in peptide **12** was removed using $Pd(PPh_3)_4$/DMBA followed by removal of the Fmoc group on Ser11 to give peptide **13**. Cyclization of peptide **13** to give peptide **14** was accomplished using PyAOP/HOAT/2,4,6-collidine in 3:1 DMF:dichloromethane containing 1% Triton™ X-100. Cleavage from the resin using a TFA:TIPS:H_2O cleavage cocktail gave peptide **1**. The same route was used for peptide **2**. Both were purified by reversed-phase HPLC.

ent-Dap-K6-E12-W13 was prepared in exactly the same manner as Dap-K6-E12-W13, except that the amino acid building blocks employed were of the opposite stereochemistry.[23] The enantiomeric peptides had identical analytical RP-HPLC retention times and the chromatogram resulting from a coinjection of the two peptides exhibited a single peak (See Fig. S6 in the SI). Moreover, their circular dichroism spectra further supported their enantiomeric nature (see Fig. S7 in the SI).

2.2. Antibacterial activity of daptomycin analogs

Peptides **1** and **2** and *ent*-Dap-K6-E12-W13 were assayed against *B. subtilis* 1046 (Table 1). Analogs **1** and **2** were substantially less active than Dap-K6-E12-W13 at physiological Ca^{2+} concentration, unequivocally demonstrating that, in addition to the methyl group on the Thr side chain, the ester bond in daptomycin is indeed crucial for its activity. Analog **1** exhibited greater activity than **2** at 1.25 mM Ca^{2+}, indicating that the R-configuration (the same as in the side chain of L-Thr in daptomycin) at the 3-position of the DABA residue is preferred in these analogs. As we have found with other moderately or poorly active daptomycin analogs,[20–23] some of the activity of **1** and **2** could be regained by increasing the Ca^{2+} concentration, suggesting that amide (versus ester) bond and the configuration at the 3-position of the DABA side chain (or Thr in Dap) affects Ca^{2+} binding without changing the action mechanism of the antibiotic substantially.

ent-Dap-K6-E12-W13 was at least 133-fold less active than Dap-K6-E12-W13, which strongly indicates that a specific chiral interaction is required for daptomycin's activity. It is highly possible that the required chiral interaction involves the chiral lipid PG, whose presence in bacterial membranes is essential for daptomycin's activity. Additionally, recent studies on daptomycin's MoA suggest that a chiral interaction between daptomycin and a membrane bound protein may be required for activity.[9]

2.3. Membrane binding studies with peptides 1 and 2

The binding of daptomycin and its analogs to large unilamellar vesicles (LUV) containing PG as a function of Ca^{2+}-concentration can be examined by monitoring the change in the intrinsic fluorescence of the Kyn and/or Trp residue(s).[23,31] Fig. 3 shows the membrane binding curves for daptomycin, Dap-K6-E12-W13, peptides **1** and **2**, and *ent*-Dap-K6-E12-W13 using LUVs composed of equimolar quantities of dimyristoylphosphatidylcholine (DMPC) and dimyrisitoylphosphatidylglycerol (DMPG).

For daptomycin and Dap-K6-E12-W13, the fluorescence increased sharply when the concentration of Ca^{2+} exceeded 0.1 mM indicating insertion of the Kyn (daptomycin) or Trp (Dap-K6-E12-W13) residues into the membrane. The signal approaches saturation at approximately 1 mM Ca^{2+}. In contrast, for peptide **1**, the fluorescence did not increase sharply until the concentration of Ca^{2+} exceeded 1 mM and did not approach saturation until approximately 50 mM Ca^{2+}. For peptide **2**, the fluorescence increased sharply when the concentration of Ca^{2+} exceeded 10 mM and did not approach saturation until approximately 100 mM Ca^{2+}. These results suggest that peptides **1** and **2** have a lower affinity for Ca^{2+} than Dap-K6-E12-W13 and/or the **1**-Ca^{2+} and **2**-Ca^{2+} complexes have a lower affinity for the liposomes than the Dap-K6-E12-W13-Ca^{2+} complex. In any case, the reduced affinities of these peptides for Ca^{2+} and/or the reduced affinity of their Ca^{2+} complexes for the target membranes may be the reason for the reduced activity of these analogs.

The membrane binding curves of Dap-K6-E12-W13 and *ent*-Dap-K6-E12-W13 differ significantly in that approximately 10 times more Ca^{2+} is required for complete insertion of *ent*-Dap-K6-E12-W13 into the membrane compared to Dap-K6-E12-W13: Dap-K6-E12-W13 begins to respond to Ca^{2+} at approximately 0.1 mM with maximal intensity obtained at approximately 1 mM while *ent*-Dap-K6-E12-W13 begins to respond to Ca^{2+} at approximately 0.3 mM with maximal intensity obtained at approximately 10 mM. Being enantiomers, the intrinsic calcium affinity of Dap-K6-E12-W13 and *ent*-Dap-K6-E12-W13 must be the same. Hence, the disparity in their membrane binding curves must be due to the difference in the affinity of their Ca^{2+} complexes for PG.[32] This strongly suggests that the stereochemistry of PG effects

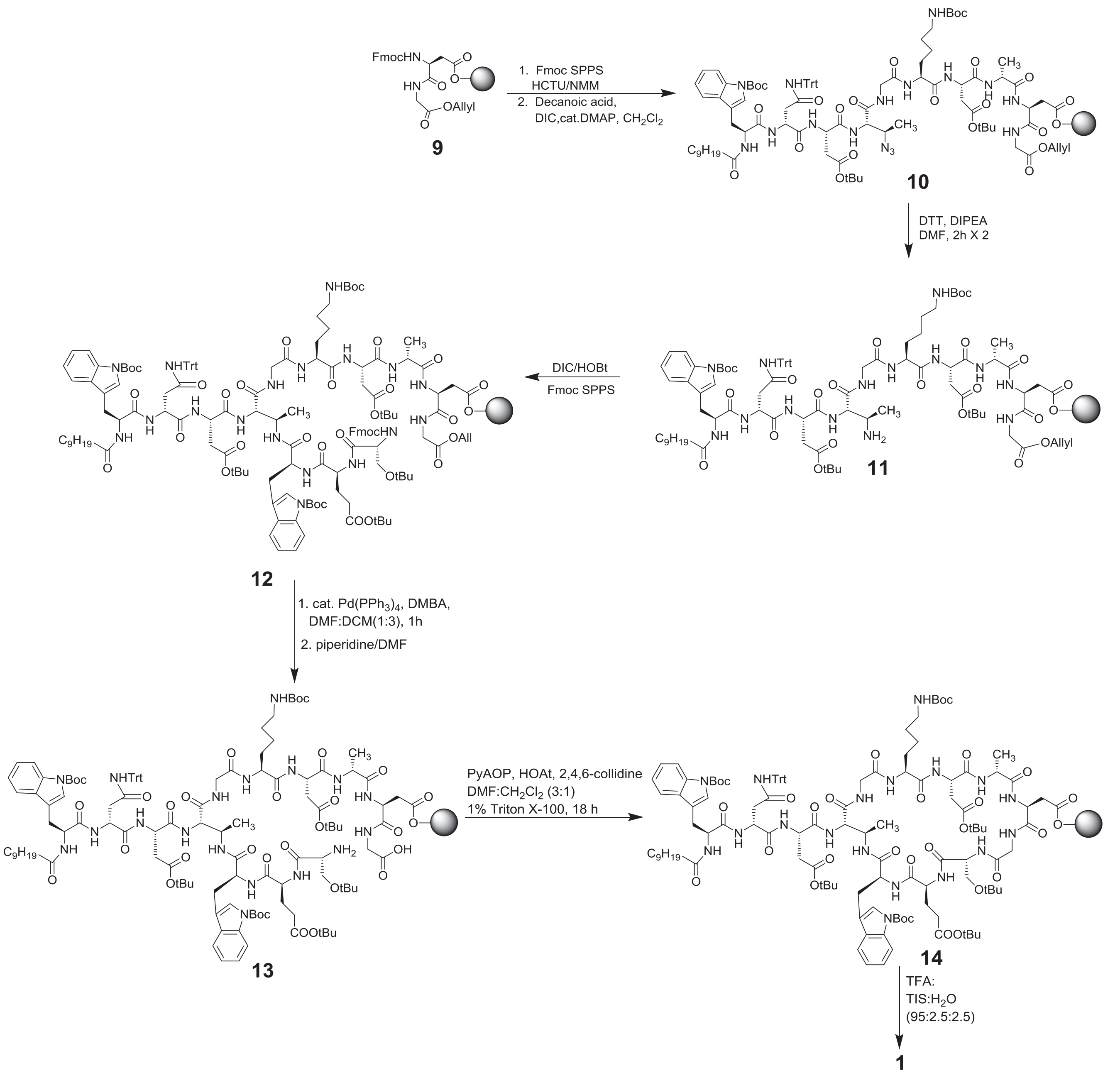

Scheme 2. Synthesis of peptide **1**. The synthesis of peptide **2** was accomplished in an identical manner using (2*S*,3*S*)-FmocAABA (**8**).

Table 1
MIC values of daptomycin and its analogs against *B. subtilis* 1046.

Peptide	MIC (μg/mL) 1.25 mM Ca^{+2}	5 mM Ca^{+2}
Dap	0.75	0.5
Dap-K6-E12-W13	1.5	0.5
1	50	10
2	> 100	10
ent-Dap-K6-E12-W13	> 200	100

daptomycin-membrane interactions. It is important to note that the commercial DMPG used in this study, 1,2-dimyristoyl-*sn*-glycero-3-phospho-(1′-*rac*-glycerol), was a 1:1 mixture of *R*,*R* and *R*,*S* diastereomers. Therefore, it is possible that the effect of the PG stereochemistry on daptomycin-membrane interactions is even greater than what is shown in Fig. 3. To the best of our knowledge, the absolute configuration at both stereogenic centers in PG in *B. subtilis* membranes has not been unequivocally established.

3. Conclusions

In this report we have demonstrated that, in addition to the methyl group on the Thr side chain, the ester bond in daptomycin is also crucial for daptomycin's activity. Moreover, we have also shown that, since the enantiomer of Dap-K6-E12-W13 is inactive, a specific chiral interaction (s) is required for daptomycin's activity. We also provide evidence that daptomycin is involved in a chiral interaction with PG. Membrane binding studies with Dap-K6-E12-W13 and *ent*-Dap-K6-E12-W13 using liposomes made up of the individual stereoisomers of PG would enable one to provide a more complete picture of the effect of PG stereochemistry on daptomycin-membrane interactions. Such studies are in progress and will be reported in due course.

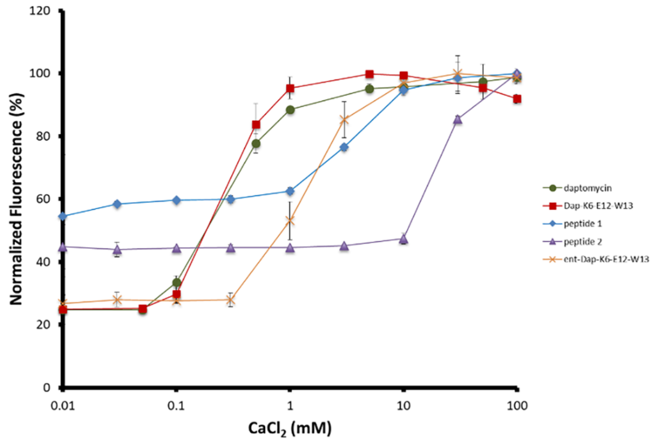

Fig. 3. The intrinsic fluorescence of daptomycin (green), Dap-K6-E12-W13 (red) and peptide **1** (blue), peptide **2** (purple) and *ent*-Dap-K6-E12-W13 (orange) in the presence of DMPC/DMPG (1:1) LUVs as a function of Ca^{2+} concentration. An increase in the intrinsic fluorescence of the Kyn residue in daptomycin or of the Trp residues in Dap-K6-E12-W13, peptide **1**, peptide **2** and *ent*-Dap-K6-E12-W13 indicates insertion of the fluorophore. The data shown was normalized by the maximum emission intensity observed in each titration, with error bars representing the standard deviations of three separate experiments.

4. Experimental

4.1. General methods

All resins, amino acids and reagents were purchased from commercial suppliers. ACS grade *N,N*-dimethylformamide (DMF) was dried by distillation over calcium hydride under reduced pressure. Dichloromethane and acetonitrile were dried by distillation over calcium hydride under nitrogen. Pyridine was dried by refluxing over potassium hydroxide followed by fractional distillation. Tetrahydrofuran (THF) was distilled from sodium metal in the presence of benzophenone under N_2. Chromatography was preformed using 60 Å silica gel.

All peptide syntheses were performed manually using a rotary shaker for agitation.[23] *ent*-Dap-K6-E12-W13 was prepared using the same procedure that was used for preparing Dap-K6-E12-W13 (see Figs. S5–S7 for the HRMS, analytical HPLC and CD spectrum of *ent*-Dap-K6-E12-W13).[23] Membrane binding studies and MIC determinations were performed as previously described.[23]

Reversed-phase analytical and semi preparative HPLC were performed using a Waters 600 controller equipped with Waters 2487 dual wavelength detector set to 220 and 260 nm. A Higgins Analytical Inc. (Mountainview, CA, USA) CLIPEUS C18 column (10 µM, 250 × 4.6 mm) was used for analytical HPLC at a flow rate of 1 mL/min. Reversed-phase semi-preparative HPLC was performed using a Higgins CLIPEUS C18 column (10 µM, 250 × 20 mm) at a flow rate of 10.0 mL/min.

Circular dichroism traces were collected using a Jasco J − 715CD spectrometer. The peptide concentration of each solution was 100 µM in 20 mM HEPES buffer (pH 7.4). Samples were measured at room temperature from 210 − 250 nm at a scan rate of 50 nm min^{-1} and a bandwidth 1 nm. A 1 mm cuvette was used. The outputted data was converted to molar ellipticity in units of deg cm^2 $dmol^{-1}$.

High resolution positive electrospray (ESI) mass spectra were obtained using an orbitrap mass spectrometer. Samples were sprayed from MeOH: 1% formic acid in H_2O. All spectra were collected in the positive mode. ^1H- and ^{13}C NMR were collected using a Bruker Avance-300 spectrophotometer. Chemical shifts (δ) for samples run in $CDCl_3$ are reported in ppm relative to an internal standard (trimethylsilane, δ 0). For ^{13}C NMR samples run in $CDCl_3$ chemical shifts are reported relative to the residual solvent peak (77.0 ppm). Chemical shifts (δ) for samples run in CD_3OD are reported relative to the residual solvent peak (δ 3.30). For ^{13}C NMR samples run in CD_3OD, chemical shifts are reported relative to the residual solvent peak (49.15 ppm, central peak).

4.2. Syntheses

4.2.1. *Di-tert-butyl (4S,5R)-5-methyl-1,2,3-oxathiazolidine-3,4-dicarboxylate 2,2-dioxide* (**3**) *and di-tert-butyl (4S,5S)-5-methyl-1,2,3-oxathiazolidine-3,4-dicarboxylate 2,2-dioxide* (**6**)

Anhydrous acetonitrile (14 mL) and thionyl chloride (1.38 mL, 19.1 mmol, 2.05 equiv) were added to a reaction vessel at − 5 °C. Boc-L-ThrOtBu[29] (2.56 g, 9.31 mmol, 1 equiv) in anhydrous acetonitrile (7 mL) was added dropwise to the reaction vessel. Anhydrous pyridine (3.75 mL, 46.6 mmol, 5 equiv) was then added dropwise to the stirred mixture. After 10 min, cooling was removed, the reaction was stirred at room temperature for 3 h, then concentrated. The residue was mixed with ethyl acetate (65 mL) and water (18 mL) and stirred at room temperature for 20 min. The aqueous layer was extracted with ethyl acetate (65 mL) once then the combined organic layers were washed with brine (150 mL) 3 times, then concentrated. The residue was dissolved in acetonitrile (18 mL) at room temperature and cooled using an ice bath. Ruthenium (III) chloride was added (4 mg, 0.02 mmol, 0.002 equiv), followed by sodium periodate (3.98 g, 18.62 mmol, 2 equiv). After stirring for 10 min, water (18 mL) was added dropwise, cooling was removed, and the mixture was stirred for 1.5 h at room temperature. The mixture was filtered, washed with brine (18 mL) once and extracted with ethyl acetate (18 mL) twice. The organic layer was washed with brine (50 mL) once, dried over Na_2SO_4, filtered over a bed of Na_2SO_4 + silica gel + celite then concentrated, yielding **3** as an orange oil (2.59 g, 82% yield). ^1H NMR (300 MHz, $CDCl_3$) δ 4.81 (1H, q, J = *5.8* Hz) 4.33 (1H, d, J = *5.5* Hz) 1.69 (1H, d, J = *6.4* Hz) 1.55 (9H, s) 1.49 (9H, s). ^{13}C NMR (99 MHz, $CDCl_3$) δ 165.4, 148.2, 85.7, 84.2, 77.5, 64.3, 27.8, 19.1. HRMS-ESI$^+$ (*m/z*) calcd for $C_{13}H_{24}NO_7S$ $(M+H)^+$, 338.12680; found, 338.12632.

6 was prepared using the same procedure starting from Boc-L-*allo*-ThrOtBu (74% yield). ^1H NMR (300 MHz, $CDCl_3$) δ 5.05 (1H, q, J = *6.3* Hz) 4.46 (1H, d, J = *6.0* Hz) 1.56–1.44 (21H, m). ^{13}C NMR (99 MHz, $CDCl_3$) δ 164.8, 148.0, 85.5, 84.0, 76.0, 62.9, 27.8, 15.1. HRMS-ESI$^+$ (*m/z*) calcd for $C_{13}H_{27}N_2O_7S$ $(M+NH_4)^+$, 355.15335; found, 355.15337.

4.2.2. *tert-butyl (2S,3S)-3-azido-2-((tert-butoxycarbonyl)amino)butanoate* (**4**) *and tert-butyl (2R,3S)-3-azido-2-((tert-butoxycarbonyl)amino) butanoate* (**7**)

To a solution of **3** (2.56 g, 7.67 mmol, 1 equiv) in anhydrous DMF (28 mL) at − 40 °C was added sodium azide (650 mg, 9.97 mmol, 1.3 equiv) portion wise. The mixture was allowed to reach room temperature over 4 h, at which point 20% $NaCl_{(aq)}$ (17 mL) and 2 N H_2SO_4 (1.7 mL) were added. The reaction mixture was stirred at room temperature for 3 h, then partitioned between ethyl acetate (75 mL) and water (200 mL). The aqueous layer was extracted with ethyl acetate (75 mL) once. The combined organic layers were washed with water (150 mL) once and brine (150 mL) once, dried over Na_2SO_4, then concentrated yielding **4** as a yellow oil (2.06 g, 84% yield). ^1H NMR (300 MHz, $CDCl_3$) δ 5.28 (1H, br. s.) 4.32–4.29 (1H, m) 3.78 (1H, m) 1.53 (9H, s) 1.45 (9H, s) 1.33 (3H, d, J = *6.8* Hz). ^{13}C NMR (99 MHz, $CDCl_3$) δ 168.5, 155.1, 83.0, 80.2, 58.9, 57.9, 28.2, 27.9, 15.4. HRMS-ESI$^+$ (*m/z*) calcd for $C_{13}H_{25}N_4O_4$ $(M+H)^+$, 301.18629; found, 301.18629.

7 was prepared using the same procedure starting from **6** (94% yield). ^1H NMR (300 MHz, $CDCl_3$) δ 5.10 (1H, d J = *9.1 Hz*) 4.23 (1H, d J = *8.7 Hz*) 4.10–4.08 (1H, m) 1.47 (9H, s) 1.44 (9H, s) 1.33 (3H, d, J = *6.7* Hz). ^{13}C NMR (99 MHz, $CDCl_3$) δ 169.0, 155.8, 82.6, 79.8, 58.9, 57.6, 28.1, 27.8, 16.0. HRMS-ESI$^+$ (*m/z*) calcd for $C_{13}H_{24}KN_4O_4$ $(M+K)^+$, 339.14166; found, 339.14291.

*4.2.3. (2S,3S)-2-((((9H-fluoren-9-yl)methoxy)carbonyl)amino)-3-azidobutanoic acid (**5**) and (2R,3S)-2-((((9H-fluoren-9-yl)methoxy)carbonyl)amino)-3-azidobutanoic acid (**8**)*

A reaction vessel containing **4** (2.06 g, 6.87 mmol, 1 equiv) was cooled in an ice bath then trifluoroacetic acid (15 mL) and water (2 mL) were added dropwise. The ice bath was removed and the mixture stirred for 2 h. The mixture was concentrated and residual TFA was removed by several rotary evaporations with toluene. The residue was suspended in water (33 mL), then cooled in an ice bath and basified slowly with sodium carbonate to a pH of 8 over a period of 30 min. A solution of *N*-(9-fluorenylmethoxycarbonyloxy)succinimide (FmocOsu) (2.55 g, 7.56 mmol, 1.1 equiv) in THF (18 mL) was added dropwise to the stirring reaction mixture to avoid clumping of the formed precipitate. Once the addition was complete, the ice bath was removed and the mixture stirred for 16 h. Two-thirds of the solvent was removed and the residue was acidified with concentrated HCl to a pH of 2. Dichloromethane (20 mL) was then added to the residue and the mixture was stirred for 10 min. The aqueous layer was then extracted with dichloromethane (20 mL) once and the combined organic layers were dried over Na_2SO_4, concentrated and subjected to silica gel column chromatography (98:1:1 dichloromethane:AcOH:MeOH), which gave **5** as a white powder (1.86 g, 74% yield). NMR data was found to match that reported in literature.[27] ^{1}H NMR (300 MHz, CD_3OD) δ 7.76 (2H, d, $J = 7.4$ Hz) 7.65 (2H, d, $J = 7.4$ Hz) 7.39–7.34 (2H, m) 7.31–7.26 (2H, m) 4.44–4.30 (3H, m) 4.22–4.18 (1H, m) 3.89 (1H, quintet, $J = 6.3$ Hz) 1.29 (3H, d, $J = 6.8$ Hz). ^{13}C NMR (99 MHz, CD_3OD) δ 174.7, 158.7, 145.4, 145.3, 142.7, 128.9, 128.3, 126.4, 121.1, 68.4, 59.3, 59.2, 48.5, 15.4. HRMS-ESI$^+$ (*m/z*) calcd for $C_{19}H_{19}N_4O_4$ $(M+H)^+$, 367.14008; found, 367.14000.

8 was prepared using the exact same procedure starting from **7** (74% yield). NMR data was found to match that reported in literature.[27] ^{1}H NMR (300 MHz, CD_3OD) δ 7.78 (2H, d, $J = 7.4$ Hz) 7.68 (2H, d, $J = 7.4$ Hz) 7.40–7.35 (2H, m) 7.32–7.27 (2H, m) 4.87–4.31 (3H, m) 4.26–4.21 (1H, m) 3.89 (1H, quintet, $J = 6.3$ Hz) 1.29 (3H, d, $J = 6.8$ Hz). ^{13}C NMR (99 MHz, CD_3OD) δ 173.1, 159.1, 145.4, 145.2, 142.7, 128.9, 128.3, 126.4, 121.1, 68.3, 59.7, 59.4, 48.5, 16.7. HRMS-ESI$^+$ (*m/z*) calcd for $C_{19}H_{19}N_4O_4$ $(M-H)^+$, 367.14008; found, 367.13998.

*4.2.4. Synthesis of peptide **1** and **2***

For the synthesis of peptides **1** and **2**, in addition to compounds **5** and **8**, the following protected amino acids were used: FmocAsp(tBu)OH, FmocGlyOH, FmocGlu(tBu)OH, FmocTrp(Boc)OH, Fmoc-D-Ser(tBu)OH, FmocLys(Boc)OH, Fmoc-D-AlaOH, Fmoc-D-Asn(Trt)OH, FmocTrp(Boc)OH. Chlorotrityl chloride Tentagel resin (2ClTrt-TG, 1052 mg, 0.19 mmol/g) was swollen in dichloromethane (3 × 15 min). To the swollen resin was added FmocAspGlyOallyl[23] (4.0 equiv) and diisopropylethylamine (DIPEA) (8.0 equiv) as solution in dichloromethane (3.5 mL). After agitating for 4 h, the resin was filtered and washed with dichloromethane (15 min × 3) and the resin was capped using dichloromethane:MeOH: DIPEA (1.5 mL, 17:2:1, 3 × 15 min). The capped resin was washed with dichloromethane (3 min × 3) followed by DMF (3 min × 3). Following deprotection using 2-methylpiperidine (20% in DMF, 1 × 5 min, 1 × 15 min) and washing with DMF (3 min × 3), all subsequent residues (5 equiv for each coupling) were coupled on using [(6-chloro-1*H*-benzotriazol-1-yl)oxy](dimethylamino)-*N,N*-dimethylmethaniminium hexafluoro-phosphate (HCTU) (5 equiv) and *N*-methylmorpholine (5 equiv) as a solution in DMF (3.5 mL). All couplings were found to go to completion after 50 min, at which point the resin was filtered and washed with DMF (3 min × 3). The decanoyl tail was added by coupling decanoic acid (4 equiv) to Trp at position 1 using DIC/HOBt for 13 h. Once the resin was washed, the azide on the AABA residue at position 4 was reduced to the corresponding amine by agitating the resin in a solution of dithiothreitol (2 M) and DIPEA (1 M) for 2 h two times. The remaining residues were coupled onto the resulting amine using DIC/HOBt (5equiv) in DMF (3.5 mL). The allyl group on Gly at position 10 was removed using catalytic $Pd(PPh_3)_4$ (0.2 equiv) and 1,3-dimethylbarbituric acid (DMBA, 10 equiv) in DMF:dichloromethane (1.5 mL, 1:3). The resin was washed with dichloromethane (3 × 3 min), then a 1.0% solution of sodium diethyldithiocarbamate trihydrate in DMF (3 × 3 min) to remove excess Pd catalyst, and then dichloromethane (3 × 3 min) and DMF (3 × 3 min). Following Fmoc-deprotection of Ser at position 11, the linear peptide was cyclized using (7-azabenzotriazol-1-yloxy)tripyrrolidinophosphonium hexafluorophosphate (PyAOP)/1-Hydroxy-7-azabenzotriazole (HOAT)/2,4,6-collidine (4:4:8 equiv) with 1% Triton-X 100 in DMF (4 mL). The resulting peptide was simultaneously cleaved from the resin and globally deprotected using TFA:triisopropylsilane (TIPS):H_2O 95:2.5:2.5. The crude peptide was concentrated under a stream of air and purified by semi-preparatory HPLC. Peptide **1** (16 mg, 10% yield): purified using 65:35 ACN:0.1% TFA in H_2O for 50 min (t_r = 29.6 min), HRMS-ESI$^+$ (*m/z*) calcd for $C_{73}H_{103}N_{18}O_{24}$ $(M+H^+)$, 1615.7387; found, 1615.7378. Peptide **2** (8 mg, 5%): purified using 65:35 ACN:0.1% TFA in H_2O for 50 min (t_r = 32.6 min), HRMS-ESI$^+$ (*m/z*) calcd for $C_{73}H_{103}N_{18}O_{24}$ $(M+H^+)$, 1615.7387; found, 1615.7392 (See Figs. S1–S4 in the SI for analytical HPLC chromatograms and HRMS).

Acknowledgment

This work was supported by Natural Sciences and Engineering Research Council of Canada (NSERC) Discovery grants to S.D.T. (04233-2017) and M.P. (250265-2013). R.M. is grateful to NSERC for a post-graduate scholarship. G.B. is grateful to the Government of Saudi Arabia for the King Abdullah Bin Abdulaziz Scholarship.

Appendix A. Supplementary data

Supplementary data to this article can be found online at https://doi.org/10.1016/j.bmc.2018.12.004.

References

1. Vilhena C, Bettencourt A. Daptomycin: a review of properties, clinical use, drug delivery and resistance. *Mini Rev Med Chem.* 2012;12:202–209.
2. Critically important antimicrobials for human medicine – 3rd revision. Geneva, Switzerland: WHO Press, World Health Organization; 2012.
3. For a review on daptomycin resistance mechanisms see: Tran TT, Munita JM, Arias CA. Mechanisms of drug resistance: daptomycin resistance. *Ann NY Acad Sci.* 2015;1354:32–53.
4. For a review that focusses on the mechanism of action of daptomycin see: Taylor SD, Palmer M. *Bioorg Med Chem.* 2016;24:6253–6268.
5. Canepari P, Boaretti M, Lleó MM, Satta G. Lipoteichoic acid as a new target for activity of antibiotics: mode of action of daptomycin (LY146032). *Antimicrob Agents Chemother.* 1990;34:1220–1226.
6. Allen NE, Alborn WE, Hobbs JN. Inhibition of membrane potential-dependent amino acid transport by daptomycin. *Antimicrob Agents Chemother.* 1991;35:2639–2642.
7. Allen NE, Alborn WE, Preston DA. Daptomycin disrupts membrane potential in growing *Staphylococcus aureus*. *Antimicrob Agent Chemother.* 1991;35:2282–2287.
8. Silverman JA, Perlmutter NG, Shapiro HM. Correlation of daptomycin bactericidal activity and membrane depolarization in *Staphylococcus aureus*. *Antimicrob Agents Chemother.* 2003;47:2538–2544.
9. Muraih JK, Palmer M. Estimation of the subunit stoichiometry of the membrane-associated daptomycin oligomer by FRET. *Biochim Biophys Acta Biomembr.* 2012;1818:1642–1647.
10. Zhang T, Muraih JK, Mintzer E, et al. Mutual inhibition through hybrid oligomer formation of daptomycin and the semisynthetic lipopeptide antibiotic CB-182,462. *Biochim Biophys Acta Biomembr.* 2013;1828:302–308.
11. Muraih JK, Harris J, Taylor SD, Palmer M. Characterization of daptomycin oligomerization with perylene excimer fluorescence: stoichiometric binding of phosphatidylglycerol triggers oligomer formation. CB-182,462. *Biochim Biophys Acta Biomembr.* 2012;1818:673–678.
12. Zhang T, Muraih JK, MacCormick B, Silverman J, Palmer M. Daptomycin forms cation- and size-selective pores in model membranes. *Biochim Biophys Acta Biomembr.* 2014;1838:2425–2430.
13. Zhang TH, Muraih JK, Tishbi N, et al. Cardiolipin prevents membrane translocation and permeabilization by daptomycin. *J Biol Chem.* 2014;289:11584–11591.
14. Muller A, Wenzel M, Strahl H, et al. Daptomycin inhibits cell envelope synthesis by interfering with fluid membrane microdomains. *Proc Natl Acad Sci USA.* 2016;113:E7077–E7086.

15. In addition to these two mechanisms, other mechanisms have been proposed. See ref. 4.
16. Baltz RH. Daptomycin and A54145: structure-activity relationship (SAR) studies enabled by combinatorial biosynthesis. In: Osbourn A, Goss RJ, Carter GT, eds. *Natural Products: Discourse, Diversity, and Design.* John Wiley & Sons, Inc.; 2014 Chapter 23.
17. Grunewald J, Marahiel MA. Chemoenzymatic and template-directed synthesis of bioactive macrocyclic peptides. *Microbiol Mol Biol Rev.* 2006;70:121–146.
18. Lam HY, Zhang Y, Liu H, et al. Total synthesis of daptomycin by cyclization via a chemoselective serine ligation. *J Am Chem Soc.* 2013;135:6272–6279.
19. Lohani CR, Taylor R, Palmer M, Taylor SD. Solid-phase total synthesis of daptomycin and analogs. *Org Lett.* 2015;17:748–751.
20. Lohani CR, Taylor R, Palmer M, Taylor SD. Solid-phase synthesis and in vitro biological activity of a Thr4→Ser4 analog of daptomycin. *Bioorg Med Chem Lett.* 2015;25:5490–5494.
21. Lohani CR, Rasera B, Scott B, Palmer M, Taylor SD. α-Azido acids in solid phase peptide synthesis: compatibility with fmoc chemistry and an alternative approach to the solid phase synthesis of daptomycin analogs. *J Org Chem.* 2016;81:2624–2628.
22. Barnawi G, Noden M, Taylor R, et al. An entirely Fmoc solid phase approach to the synthesis of daptomycin analogs. *Biopolym Pept Sci.* 2018:e23094.
23. D'Costa VM, Mukhtar TA, Patel T, et al. Inactivation of the lipopeptide antibiotic daptomycin by hydrolytic mechanisms. *Antimicrob Agents Chemother.* 2012;56:757–776.
24. (a) For examples see: Sando L, Henriques ST, Foley F, et al. A synthetic mirror image of kalata B1 reveals that cyclotide activity is independent of a protein receptor. *ChemBioChem.* 2011;12:2456–2463
(b) Dettner F, Hanchen A, Schols D, Toti L, Nusser A, Sussmuth RD. Total synthesis of the antiviral peptide antibiotic feglymycin. *Angew Chem Int Ed Engl.* 2009;48:1856–1861.
25. 't Hart P, Kleijn LHJ, de Bruin G, Oppedijk SF, Kemmink J, Martin NI. A combined solid- and solution-phase approach provides convenient access to analogues of the calcium-dependent lipopeptide antibiotics. *Org Biomol Chem.* 2014;12:913–918.
26. Dianati V, Shamloo A, Kwiatkowska A, et al. Rational design of a highly potent and selective peptide inhibitor of PACE4 by salt bridge interaction with D160 at position P3. *ChemMedChem.* 2017;12:1169–1172.
27. Donnell AF, Kester R, Lou Y, Anthony J, Remiszewski S. 2-oxo-2,3,4,5-tetrahydro-1H-benzobdiazepines and their use in the treatment of cancer. US Patent, 0225449 A1; 2015.
28. Koch S, Schollmeyer D, Lçwe H, Kunz H. C-Glycosyl amino acids through hydroboration–cross-coupling of exo-glycals and their application in automated solid-phase synthesis. *Chem Eur J.* 2013;19:7020–7041.
29. Myers EL, Raines RT. A phosphine-mediated conversion of azides into diazo compounds. *Angew Chem Int Ed.* 2009;48:2359–2363.
30. Lakey JH, Ptak M. Fluorescence indicates a calcium-dependent interaction between the lipopeptide antibiotic LY146032 and phospholipid membranes. *Biochemistry.* 1988;27:4639–4645.
31. The baseline fluorescence of peptides **1** and **2** is higher than that of Dap-K6-E12-W13 and *ent*-Dap-K6-E12-W13. The difference is mainly due to the fluorophores. With Dap-K6-E12-W13 and *ent*-Dap-K6-E12-W13, kynurenine fluorescence is monitored, which has very low quantum yield (intensity) in water. With peptides **1** and **2**, tryptophan fluorescence is monitored, which tends to have a significant quantum yield in both water and membranes.
32. There is no PC requirement for Dap activity and so it is unlikely that the stereo chemistry of PC is important.